Available online at www.sciencedirect.com
ScienceDirect
Polymer 48 (2007) 2928–2938
polymer
www.elsevier.com/locate/polymer

The domain structure and mobility of semi-crystalline poly(3-hydroxybutyrate) and poly(3-hydroxybutyrate-*co*-3-hydroxyvalerate): A solid-state NMR study

Limin Zhang [a], Huiru Tang [a,b,*], Guangjin Hou [a], Yiding Shen [b], Feng Deng [a,*]

[a] *State Key Laboratory of Magnetic Resonance and Atomic and Molecular Physics, Wuhan Centre for Magnetic Resonance, Wuhan Institute of Physics and Mathematics, The Chinese Academy of Sciences, Wuhan 430071, PR China*
[b] *School of Chemical Science, Shaanxi University of Science and Technology, Xianyang, Shaanxi, PR China*

Received 1 December 2006; received in revised form 6 February 2007; accepted 6 March 2007
Available online 14 March 2007

Abstract

Solid-state NMR techniques have been employed to investigate the domain structure and mobility of the bacterial biopolymeric metabolites such as poly(3-hydroxybutyrate) (PHB) and its copolymers poly(3-hydroxybutyrate-*co*-3-hydroxyvalerate) (PHBV) containing 2.7 mol% (PHBV2.7) and 6.5 mol% (PHBV6.5) 3-hydroxyvalerate. Both single-pulse excitation with magic-angle spinning (SPEMAS) and cross-polarization magic-angle spinning (CPMAS) ^{13}C NMR results showed that these biopolymers were composed of amorphous and crystalline regions having distinct molecular dynamics. Under magic-angle spinning, ^{1}H $T_{1\rho}$ and ^{13}C T_1 showed two processes for each carbon. Proton relaxation-induced spectral editing (PRISE) techniques allowed the neat separation of the ^{13}C resonances in the crystalline regions from those in the amorphous ones. The proton spin–lattice relaxation time in the tilted rotating frame, H $T^{T}_{1\rho}$, measured using the Lee–Goldburg sequence with frequency modulation (LGFM) as the spin–locking scheme, was also double exponential and significantly longer than ^{1}H $T_{1\rho}$. The difference between H $T^{T}_{1\rho}$ for the amorphous and crystalline domains was greater than that of ^{1}H $T_{1\rho}$. Our results showed that the H $T^{T}_{1\rho}$ differences could be exploited in LGFM–CPMAS experiments to separate the signals from two distinct regions. ^{1}H spin-diffusion results showed that the domain size of the mobile components in PHB, PHBV2.7 and PHBV6.5 were about 13, 24 and 36 nm whereas the ordered domain sizes were smaller than 76, 65 and 55 nm, respectively. The results indicated that the introduction of 3-hydroxyvalerate into PHB led to marked molecular mobility enhancement in the biopolymers.

Keywords: Solid-state NMR; Poly(3-hydroxybutyrate); Poly(3-hydroxybutyrate-*co*-3-hydroxyvalerate)

1. Introduction

Polyhydroxyalkanoates (PHAs) are the biopolymeric metabolites of gram-positive and gram-negative bacteria from more than 70 different genera [1] in the form of polyesters of hydroxyalkanoates (or hydroxylated fatty acids). The biopolymers can be accumulated intracellularly up to 90% of the cell dry weight, acting as a carbon and energy reserve [2,3]. PHAs are normally biosynthesized from carbohydrate (or carbon dioxide and water) and readily degraded into hydroxycarboxylic acids, which are normal endogenous metabolites of living systems; ultimately the degradation products are water and carbon dioxide, producing no new or extra carbon dioxide loads to the environment. Therefore, PHAs are renewable, biodegradable, biocompatible and environmental friendly natural alternatives to the petroleum based materials.

* Corresponding authors. State Key Laboratory of Magnetic Resonance and Atomic and Molecular Physics, Wuhan Centre for Magnetic Resonance, Wuhan Institute of Physics and Mathematics, The Chinese Academy of Sciences, Wuhan 430071, PR China. Fax: +86 27 87199291.
E-mail addresses: huiru.tang@wipm.ac.cn (H. Tang), dengf@wipm.ac.cn (F. Deng).

0032-3861/$ - see front matter © 2007 Elsevier Ltd. All rights reserved.
doi:10.1016/j.polymer.2007.03.026

As a class of optically pure PHAs, PHB has been found widespread [4] in the living systems including the cytoplasmic membrane and cytoplasma of *Escherichia coli*, in the membrane of yeast, plants and animals. Upon biodegradation, it produces 3-hydroxybutyrate (3HB), which is a mammalian endogenous metabolite also known as ''ketone body'' hence enabling PHB to have excellent biocompatibility particularly with the mammalian systems. Such biodegradability [5,6] and biocompatibility [7,8] together with the renewable and environmental friendly nature make PHB particularly attractive for many applications such as in biomedical materials [9], drug delivery systems [10], food packaging and biodegradable plastics [11]. With potential applications as the major driving force, many copolymers of 3HB have also been prepared *via* biosynthesis, such as poly(3-hydroxybutyrate-*co*-3-hydroxyvalerate) (PHBV). It has been found that the introduction of the medium and long side chain hydroxyl fatty acids results in pronounced changes in the physical properties of PHB especially its elasticity [8].

It is conceivable that the structural, dynamic and interaction properties of PHB and its copolymers are key factors governing their properties in biological functioning and functionality in applications. The elucidation of such properties is, therefore, fundamentally important to understand the mode of actions of these polyesters in the living organisms and the functionality in their applications. Extensive researches have been carried out on PHB and some of its copolymers using a variety of techniques including DSC [12,13], X-ray diffraction (XRD) [14,15] and NMR [16–19]. Among many physical techniques, high-resolution solid-state NMR is not only non-invasive and non-destructive method to facilitate *in situ* investigations but also able to provide information on molecular structure, dynamics and interactions of polymers, especially natural polymers [20–22].

XRD results have shown that PHB and PHBV (Fig. 1) have similar crystalline structures; both have 2_1 helical conformations with the fiber periods of 0.596 and 0.556 nm, respectively [23]. The crystallinity of PHBV was in the range from 62% to 69% depending on the HV concentration and decreased with the increase of 3-hydroxyvalerate (HV) content [24]. DSC results [25] showed that, compared with PHB, PHBV has lower glass transition temperature (T_g), melting point (T_m) and crystallinity. PHBV also showed reduced brittleness and enhanced elasticity [8], which may be related to their different microstructural and molecular dynamic properties.

Solid-state NMR studies revealed that the degree of crystallinity (X_c) is higher in PHB (about 70%) than PBHV and some discrepancy was evident in X_c values obtained from the CPMAS and SPEMAS NMR experiments [15–18,26]. For

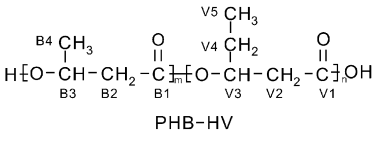

Fig. 1. Schematic representation of the chemical structural features of poly-(3-hydroxybutyrate) and poly(3-hydroxybutyrate-*co*-3-hydroxyvalerate).

both PHB and PHBV, the X_c values obtained from CPMAS NMR experiments were consistently greater than those from SPEMAS NMR [15–18,26] presumably owing to the ^1H $T_{1\rho}$ relaxation during the contact time in CPMAS NMR even though no authors have discussed about this point so far. The co-crystallization and isomorphism phenomena of PHBV containing more than 30 mol% HV have been extensively studied using high-resolution solid-state ^{13}C NMR spectroscopy and DSC [27–29]. Results showed that two crystalline phases, α-phase and β-orthorhombic phase, existed apart from the amorphous phase. PHBV containing 14–98 mol% HV has also already been studied [28,30] in terms of the co-monomer compositional distribution, thermal and morphological characteristics using WAXD, DSC and solid-state NMR. The results showed that when the HV content was lower than 47 mol%, PHBV has similar crystalline lattice to that of PHB with the HV unit as the crystal constituent whereas when the HV content was higher than 52 mol% crystalline lattice appeared to be similar to that of poly(3-hydroxyvalerate). Furthermore, whilst the T_g value of PHBV decreased consistently with the increase of 3HV content, the T_m and ΔH showed a minimum when 3HV was about 40–50 mol% [28,30]. In contrast, PHBV containing less than 14 mol% 3HV seemed to be less extensively studied. Random copolymers of P(3HB–3HV) with 0–27 mol% 3HV have been examined [31] using ^{13}C CPMAS NMR to determine the crystallinity and the partitioning of the minor fraction residues of 3HV into the crystalline region PHB-type lattice. The signals of the crystalline and those of the amorphous regions were separated according to their different $^1H_{1\rho}$ relaxation [31]. The X_c values were obtained from the amplitude of the two components by spectral deconvolution of the ^{13}C CPMAS NMR spectra. These X_c values are still expected to be overestimated due to ^1H $T_{1\rho}$ relaxation decay even during the short (0.7 ms) contact time.

Less work has been done for the PHBV containing low 3HV monomer (<10 mol%) and the structural features related to the local mobility properties of PHB/PHBV are even less researched though these properties may be important in understanding the physical properties of the biopolymers. Consequently, a number of questions remain unanswered such as 'what are the domain sizes of crystalline and amorphous regions in PHBV', 'how does 3HV content affect the domain sizes', 'what is the nature of the molecular dynamics for these domains', 'are there any relationships between the structural and dynamic properties and their macroscopic properties', if yes, 'what is the relationship'. To answer some of the questions, solid-state NMR is the method of natural choice since it can provide information in molecular structure, dynamics and interactions non-invasively and non-destructively; hence *in situ* information may be obtained. For instance, in multiple domain biopolymer systems, multiple processes are often observed for ^1H $T_{1\rho}$ and T_1 owing to inefficient spin diffusion on these time scales. This provides a unique opportunity to probe the structural and dynamic properties using proton relaxation-induced spectral editing (PRISE) techniques. It has shown as in the examples of plant cell wall systems [32] and the microstructure of native starch granules [33] that

PRISE techniques are useful not only in separating ^{13}C signals from different domains but also in revealing the structural features associated with different molecular dynamics.

In the present study, ^{13}C CPMAS, SPEMAS and PRISE NMR techniques are employed to investigate the structural characteristics of the semi-crystalline biopolymers PHB and PHBV containing 2.7 mol% and 6.5 mol% HV in different domains and dynamic states. The domain sizes and ratios are measured quantitatively. The H $T_{1\rho}^{T}$ (spin–lattice relaxation in the tilted rotating frame) has been studied for its usefulness in such systems and feasibility as a way of spectral editing. These results are interpreted in terms of their structural and molecular motional properties in the solid state.

2. Experimental section

2.1. Materials

Poly(3-hydroxybutyrate) (PHB, $M_W = 470{,}000$ g/mol) and poly(3-hydroxybutyrate-*co*-3-hydroxyvalerate) (PHBV) containing 5 wt% and 12 wt% 3-hydroxyvalerate were purchased from Aldrich Chem. Co. (Milwaukee, WI, USA, No. 80181-31-3) and used without further processing. They represent PHBV containing 0%, 2.7 mol% and 6.5 mol% HV. Our DSC results showed that the glass transition temperature (T_g) was 274, 273, 270 K and the melting temperature (T_m) was 439.7, 429.4 and 426.3 K for the PHB, PHBV2.7 and PHBV6.5, respectively. For the convenience of description, they will be referred to as PHB, PHBV2.7 and PHBV6.5, respectively, in the following discussions. All samples were dried for at least 24 h *in vacuo* at 80 °C before NMR experiments.

2.2. High-resolution solid-state NMR spectroscopy

^{13}C cross-polarization magic-angle spinning (CPMAS) and ^{13}C single-pulse excitation magic-angle spinning (SPEMAS) NMR spectra were recorded on a Varian InfinityPlus-300 NMR spectrometer equipped with a standard Chemagnetic magic-angle spinning probe head, operating at 299.98 MHz for ^{1}H and 75.12 MHz for ^{13}C, respectively. Typically, about 50 mg sample was packed into a 4 mm zirconium oxide rotor and spun at about 6 kHz (±1 Hz). For the CPMAS NMR, the Hartmann–Hahn matching condition was optimized using hexamethylbenzene (HMB). Two contact times were employed as 0.8 ms and 2 ms with the recycle delay of 6 s and proton 90° pulse length of 4.3 μs. For SPEMAS NMR, the recycle delay was selected as 30 s and 2 s, respectively, to acquire spectra with complete relaxation for some of the signals and the components with short ^{13}C T_1 relaxation time. The ^{13}C chemical shifts were referenced to a solid HMB sample externally as 17.35 ppm for the methyl groups. The ^{13}C T_1 was measured using the pulse sequence developed by Torchia [34]; the ^{1}H $T_{1\rho}$ and H $T_{1\rho}^{T}$ were measured indirectly using the CPMAS based pulse sequences [35–37] as shown in Fig. 2. All relaxation time values were obtained by curve fitting using a Levenburg–Marquardt nonlinear curve-fitting routine installed in TableCurve 2D 5.0 (AISN Software) on a personal computer. For the ^{1}H $T_{1\rho}$ and H $T_{1\rho}^{T}$ relaxation-induced spectral editing experiments, a single contact time of 0.8 ms was used. For ^{1}H $T_{1\rho}$ and H $T_{1\rho}^{T}$ partially relaxed spectra, the relaxation delay was chosen such that the short component was decayed below 1% of its initial intensity while the long components were only partially relaxed.

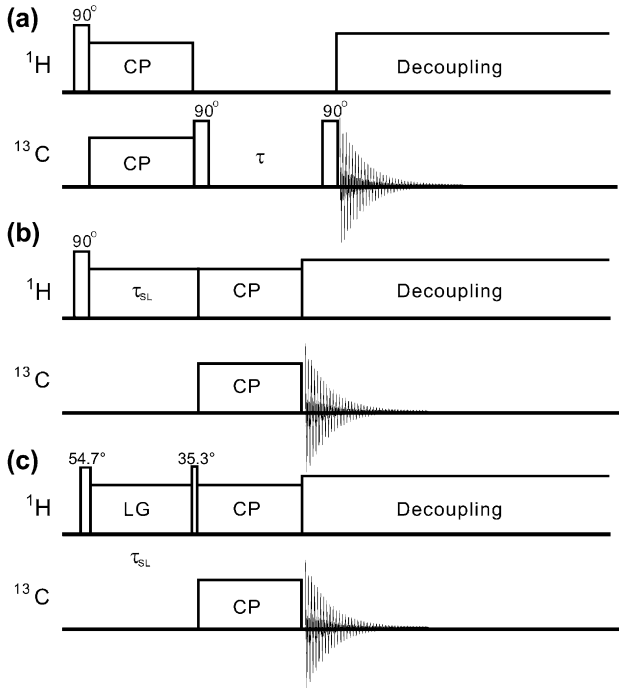

Fig. 2. The pulse sequences for measuring ^{13}C T_1 (a), ^{1}H $T_{1\rho}$ (b) and H $T_{1\rho}^{T}$ (c) of PHB and PHBV.

2.3. Measurements of crystallinity

Crystallinity (X_c) was measured by deconvoluting the ^{13}C signals of methyl groups at 21.3 ppm. The X_c values were calculated as the area percentage of the sharp peak amongst the total peak area. It has to be noted that the crystallinity so obtained included both the long range and short ranged ordered domains whereas the X-ray results included only the long range ordered structural domains.

2.4. Proton spin-diffusion measurements and domain sizes of biopolymers

The static ^{1}H solid-state NMR spectra of the samples were recorded with the same equipment as described in Section 2.2 with a single-pulse acquisition. The 90° pulse length was 4.3 μs and the recycle delay was 6 s. The proton T_2 of the mobile component (as shown in Fig. 6a) was measured using Carr–Purcell–Meiboom–Gill (CPMG) sequence [38,39], $(90_x - (\tau_E - 180_y - \tau_E)_n)$, with total relaxation delay ($2n\tau_E$) up to 10 ms.

For spin-diffusion measurements, Goldman–Shen pulse sequence [40] was employed with the inter-pulse delay of 15 μs between the first two 90° pulses to eliminate the ^{1}H magnetization of the rigid component, leaving that of the mobile one

less attenuated. After storing the remaining magnetization in z-axis for various period of mixing time (t_m), the intensity of the mobile components was measured *via* spectral deconvolution to extract spin-diffusion parameters. From the diffusion curves (Fig. 8), the initial linear points were fitted into a linear equation (e.g. $y = ax + b$) (dotted line in Fig. 8) to obtain the $(t_m^{s,0})^{1/2}$ values as the intercept of the linear decay to the horizontal axis. The domain size of the mobile components was then calculated from $(t_m^{s,0})^{1/2}$ according to Eqs. (1) and (2). It has to be noted that our assumption does not consider any interface between different domains.

3. Results and discussion

3.1. ^{13}C CPMAS NMR spectroscopy of PHB and PHBV

With contact time of 0.8 ms, ^{13}C CPMAS NMR spectrum of PHB (Fig. 3a) shows clearly resolved four resonances at 171, 69.6, 42.8 and 21.3 ppm corresponding to CO, CH, CH_2 and CH_3 groups, respectively. Close inspection reveals that these signals are all composed of a sharp signal and a broad one (see insets). The sharp ones have a line-width (at the half height) of about 40 Hz whereas the broad ones are about 120 Hz. The sharp signals probably arise from ordered structure whereas the broad ones are from the disordered structure. For clarity of discussion, they are referred to as crystalline and amorphous regions, respectively, although it has to be noted that the crystalline regions include both long and short range ordered structures. This implies that there are at least two structural domains in PHB. When the contact time of 2 ms was used, the intensity of the broad components in the PHB spectrum (Fig. 3b) is substantially attenuated (see insets). This indicates that the broad components have a ^1H $T_{1\rho}$ in the range of milliseconds, suggesting that this component is associated with the domains with substantial mobility. This also imposes a potential problem for ^{13}C CPMAS NMR methods to be used to evaluate the crystallinity of this type of biopolymers.

In principle, CPMAS NMR spectra can be used to evaluate the ratio of the biopolymers in two different domains. However, CPMAS NMR method does have some drawbacks from quantification point of view since the efficiency of polarization transfer (or cross-polarization) is dependent on the strength of C–H dipolar interactions, thus the type of carbon and its mobility, and the rate of ^1H $T_{1\rho}$ relaxation compared with the contact time especially in the case of multiple domain biopolymers. As an alternative, ^{13}C SPEMAS NMR spectroscopy can obtain a more reliable measurement of the ratios for different structural domains although a long relaxation delay (acquisition time plus recycle delay) is required in such cases. To assure the repetition time is long enough to have a fully relaxed ^{13}C NMR spectrum, the knowledge of ^{13}C T_1 relaxation time is a pre-requisite.

In our case, the ^{13}C T_1 values for both crystalline and amorphous domains were measured for PHB, PHBV2.7 and PHBV6.5 and tabulated in Table 1 together with the relative proportions of both components (f_C). It has to be noted that

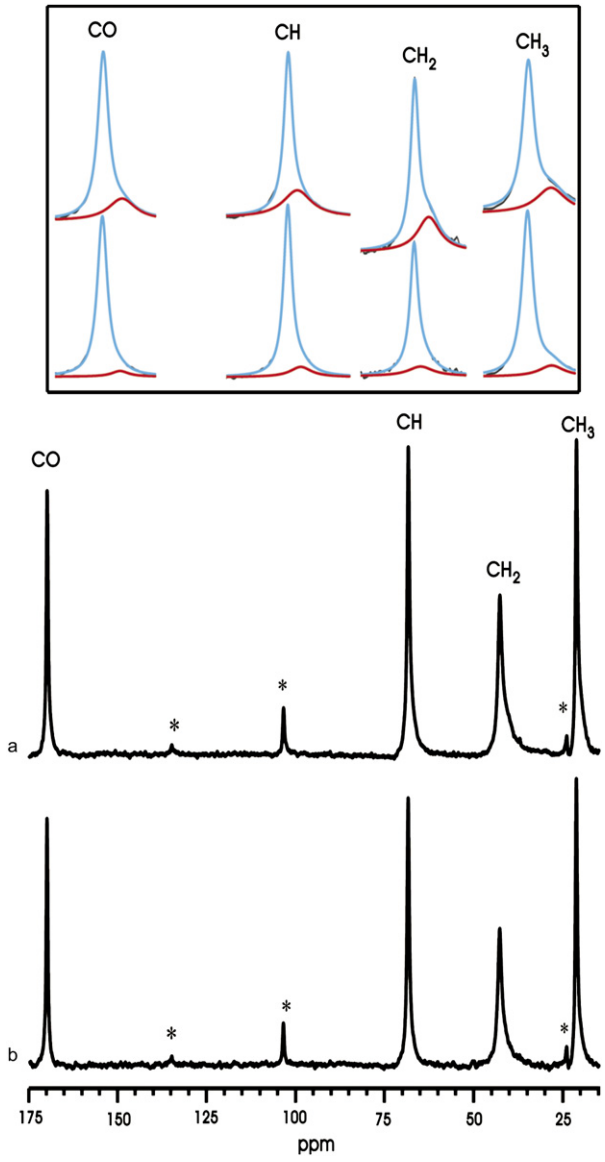

Fig. 3. ^{13}C CPMAS NMR spectra of poly(3-hydroxybutyrate) at 294 K, with contact time of (a) 0.8 ms and (b) 2 ms, at a spinning rate of 6 kHz. The asterisk denotes spin sideband. Inset shows the expansion.

the f_C values are not directly related to the number of spins in the different domains but percentage contributions to the relaxation of whole system. From the results (Table 1), it can be seen that the ^{13}C T_1 relaxation for all carbons of PHB and PHBV is double-exponential process. The long component of ^{13}C T_1, for all carbons, is about an order of magnitude longer than that of the short ones, confirming that two vastly different dynamic states are present. In addition, for all the three biopolymers in the same dynamic state, the ^{13}C T_1 values decrease steadily as a function of the number of protons attached (Table 1). This is not surprising and indicates that the ^{13}C T_1 relaxation is driven by ^{13}C–^1H dipolar interactions, which is dominated by the directly attached protons. Furthermore, PHBV samples showed shorter ^{13}C T_1 than PHB for the backbone carbons of the long T_1 components and these ^{13}C T_1 values decrease with the increase of the HV concentration (Table 1). Such

Table 1
^{1}H, ^{13}C relaxation and spin-diffusion data for PHB, PHBV2.7 and PHBV6.5 at 294 K

		PHB		PHBV2.7		PHBV6.5	
^{13}C T_1 (s)[b]	−CO	165(65%)[a]	17(35%)	115(69%)	13(31%)	110(65%)	10(35%)
	−CH	93(68%)	5.0(32%)	67(66%)	6.5(34%	59(67%)	5.8(33%)
	$-CH_2$	75(72%)	4.2(28%)	54(71%)	4.4(29%)	48(70%)	4.1(30%)
	s-CH_2(V)			39(73%)	1.8(27%)	36(75%)	1.4(25%)
	$-CH_3$(B)	2.8(79%)	0.4(21%)	4.0(81%)	0.3(19%)	4.2(80%)	0.2(20%)
	$-CH_3$(V)			4.3(82%)	0.6(18%)	4.7(83%)	0.4(17%)
^{1}H $T_{1\rho}$ (ms)[c]	−CO	98.8(67%)	6.7(33%)	90.2(68%)	5.3(32%)	89.3(69%)	4.9(31%)
	−CH	70.5(71%)	3.3(29%)	64.4(72%)	2.8(28%)	57.4(73%)	2.5(27%)
	$-CH_2$	70.6(70%)	4.2(30%)	65.2(69%)	3.7(31%)	60.3(71%)	3.3(29%)
	s-CH_2(V)			69(73%)	3.3(27%)	61.6(72%)	2.8(28%)
	$-CH_3$(B)	77.4(80%)	5.9(20%)	70.5(77%)	5.4(23%)	63.5(74%)	4.7(26%)
	$-CH_3$(V)			67.5(81%)	2.5(19%)	59.3(82%)	2.3(18%)
H $T_{1\rho}^{T}$ (ms)[d]	−CO	471.6(58%)	21.5(42%)	417.7(66%)	21.7(34%)	409.3(65%)	26.9(35%)
	−CH	416.5(67%)	33.7(33%)	412.8(71%)	27.4(29%)	381.7(74%)	34.3(26%)
	$-CH_2$	433.2(66%)	45.2(34%)	404.5(68%)	41.6(32%)	392.9(73%)	45.2(27%)
	s-CH_2(V)			422.5(73%)	40.4(27%)	401.4(70%)	51.6(30%)
	$-CH_3$(B)	508.7(78%)	50.1(22%)	477.8(69%)	51.6(31%)	453.5(66%)	47.3(34%)
	$-CH_3$(V)			421.7(72%)	25.3(28%)	406.3(75%)	22.1(25%)
$(t_m^{s,0})^{1/2}$ ($ms^{1/2}$)		11 ± 2		20.5 ± 2		31.5 ± 1	
T_2^m (ms)[e]		0.234		0.303		0.394	
$D_{eff}^{1/2}$ ($nm/ms^{1/2}$)		1.11		1.07		1.01	
Domain size (mobile part, nm)		13 ± 2		24 ± 2		36 ± 1	
Domain size (rigid part, nm)		15–76		12–65		11–55	

[a] The component proportion (f_C) is not related to the number of spin in domain but percentage of contribution to relaxation of the whole system.
[b] The fitted errors of slow and rapid were within 8% and 5%, respectively.
[c] The fitted error was within 5%.
[d] The fitted error was within 3%.
[e] T_2 of the mobile component.

^{13}C T_1 depression resulting from the introduction of HV can be attributable to two possibilities, namely, weakening of the C–H dipolar interactions and enhancement of the molecular mobility. Since addition of HV in the polymeric assembly will not affect the existing C–H bond length in PHB, which determines the C–H dipolar interactions, the enhancement of molecular mobility is probably the major reason behind the above observation. The changes for the short ^{13}C T_1 components upon the introduction of HV unit were less drastic. Assessments of the ratios of such dynamic states are important from structure–property relationship point of view.

3.2. Crystallinity for PHB and PHBV

Since solid-state NMR is sensitive to both short range and long range ordered structures, the crystalline phase discussed here will include both, thus the crystallinity measured here will also include contributions of both such long and short range ordered phases. As discussed earlier, when used to estimate the crystallinity of our biopolymers, ^{13}C CPMAS NMR spectra may lead to an overestimation since the ^{1}H $T_{1\rho}$ relaxation for the mobile components was much faster ($T_{1\rho} \sim 3$–7 ms) than that of the crystalline regions ($T_{1\rho} \sim 77$–98 ms) (see Table 1). For SPEMAS NMR, on the other hand, with some of the ^{13}C T_1 values well exceeding 100 s, an extremely long recycle delay (>500 s) has to be used to obtain fully relaxed thus quantitative ^{13}C NMR spectra. Alternatively, a small pulse angle may have to be used to sacrifice the signal-to-noise ratios. Nevertheless, since the side chain methyl groups are all relaxed much faster (~5 s) (Table 1) and its signals are all well resolved from others, methyl group signals can be employed to conduct such quantitative assessment with no necessity to wait for other carbons to relax completely. Furthermore, it is expected that methyl group ought to be in the same domain as the bulk backbone since methyl group is only one C–C bond away from the backbone whereas domain sizes are much greater for both crystalline and amorphous domains. Based on such thoughts, quantitative estimation of domain ratios was carried out only from the peak of the side chain methyl group. In our case, therefore, the SPEMAS NMR spectra were measured conveniently with a pulse repetition time of 30 s. The domain ratios of our samples were quantified by deconvolution of methyl groups as shown in Fig. 4. The ratios of the crystalline domain or X_c values are about $68 \pm 2\%$, $60 \pm 2\%$ and $56 \pm 2\%$ for PHB, PHBV2.7 and PHBV6.5, respectively. The literature reported X_c values were 81% for PHB from CPMAS NMR [31] and $64 \pm 5\%$ from the X-ray data [41]. Such values have been reported as 74% and 72% for PHBV4.4 and PHBV6.7 from CPMAS NMR [32]. The X_c value for PHBV10 [41] was $61 \pm 5\%$ from X-ray data. Furthermore, our results of X-ray analysis were $60 \pm 2\%$, $55 \pm 2\%$ and $53 \pm 2\%$ for PHB, PHBV2.7 and PHBV6.5, respectively. The X_c values of XRD, which was only sensitive to long range ordered structure, were lower than above SPEMAS NMR data.

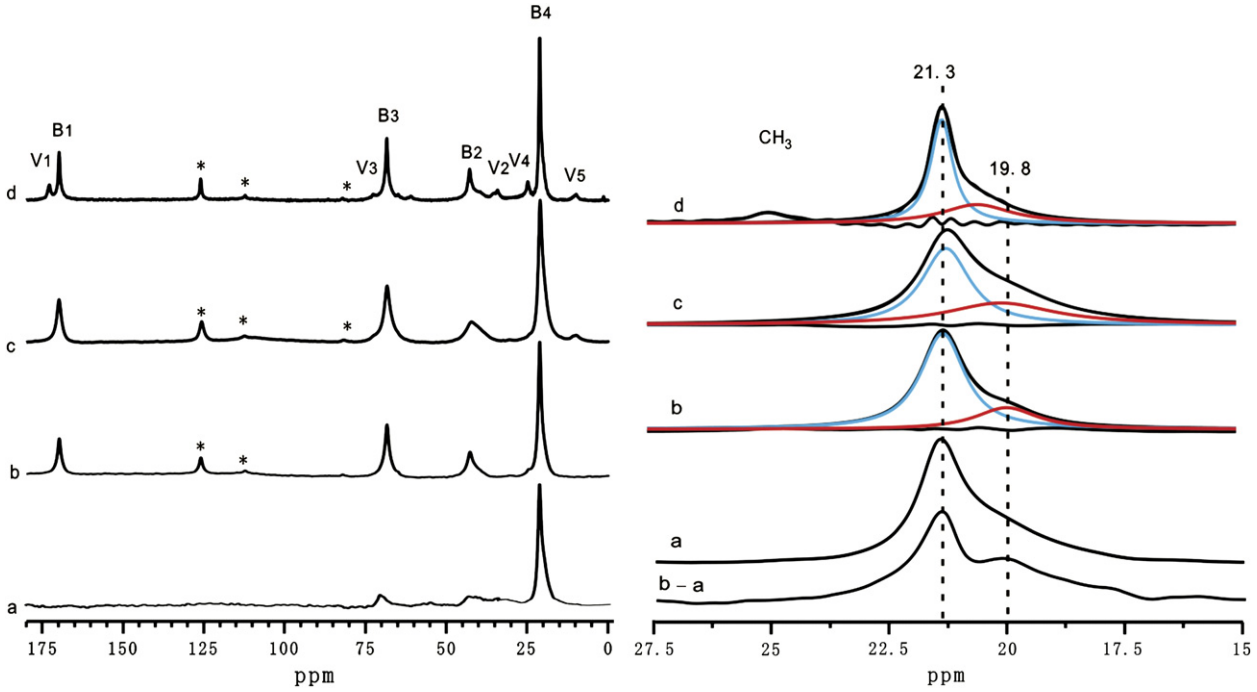

Fig. 4. ^{13}C SPEMAS NMR spectra of (a) PHB with recycle delay of 2 s and (b) PHB (c) PHBV2.7 and (d) PHBV6.5 with recycle delay of 30 s and the subtraction of (b − a). The blue and red peaks denote resonant signals associated with amorphous and crystalline components, respectively. (For interpretation of the references to colour in this figure legend, the reader is referred to the web version of this article.)

The X_c value for PHB from our SPEMAS NMR is clearly smaller than the results from the CPMAS NMR studies [31]. This can be reconciled when $T_{1\rho}$ relaxation is taken into consideration since in the previous ^{13}C CPMAS studies the amorphous ratio was underestimated due to ^{1}H $T_{1\rho}$ relaxation during the contact time. However, our results are in reasonable agreement with the X-ray results for PHB [41] though slightly higher than the X-ray results. The NMR results often showed higher ''crystallinity'' than XRD data since NMR records both long and short range ordered structures whereas the XRD reports only the long range ordered structures. Our results, being in good agreement with the X-ray data within the margin of error, suggest that these polymers have little short range ordered structure. It is worthy noting that our X_c results are also in good agreement with our DSC results (data not shown), indicating that our method is an excellent approach to measure the crystallinity. Since there are no reported X_c data for PHBV2.7 and PHBV6.5 obtained from XRD so far, we believe that our data are first accurate X_c results for these two biopolymers. From these data it is also observable that the introduction of HV co-monomer appeared to raise the ratios of amorphous structure and such ratio increase is positively correlated with the HV concentration. This is in good agreement with the previous observation that introduction of HV enhances the molecular mobility of the resultant biopolymers [42].

3.3. NMR spectral features from two domains

It is obvious from Table 1 that each carbon peak shows two distinct ^{13}C T_1 values. Although ^{13}C T_1 relaxation is largely dependent on the C−H dipolar interactions, for the similar structures in the different structure domains, the same functional groups are expected to have similar C−H bond length. If the same group in different structure domains has different ^{13}C T_1 relaxation efficiency, such differences can only result from differences in mobility. Therefore, SPEMAS NMR with carefully selected recycle delays can offer some selectivity for the signals of biopolymers in different dynamics states.

When the recycle delay was 30 s, most of the resonances with short ^{13}C T_1 were completely relaxed and that with long ^{13}C T_1 were, to large extent, relaxed though not completely. On the other hand, when the recycle delay was 2 s, only these resonances with ^{13}C T_1 shorter than 2 s were present. The difference between these two spectra provides spectral information on two components. Fig. 4 shows ^{13}C SPEMAS NMR spectra of PHB with recycle delay of 2 s (Fig. 4a) and 30 s (Fig. 4b). With recycle delay of 2 s, Fig. 4a shows only some sharp resonances corresponding probably to disordered regions with exception of CH_3 signals since the rapid methyl group rotation results in much shorter T_1. Nevertheless, the sharp signal of CH_3 (21.3 ppm) was attenuated revealing the presence of the broad signals (19.8 ppm) at the relatively high field (Fig. 4b − a). This difference in ^{13}C chemical shifts of 1.5 ppm was originated from their different chemical environment. Therefore, the long ^{13}C T_1 for each peak is associated with the sharp signals hence the crystalline phase, whereas the short T_1 component is associated with the broad signals thus amorphous structure.

All three biopolymers showed double-exponential relaxation processes for the ^{1}H $T_{1\rho}$ (Table 1); the ^{1}H $T_{1\rho}$ for the

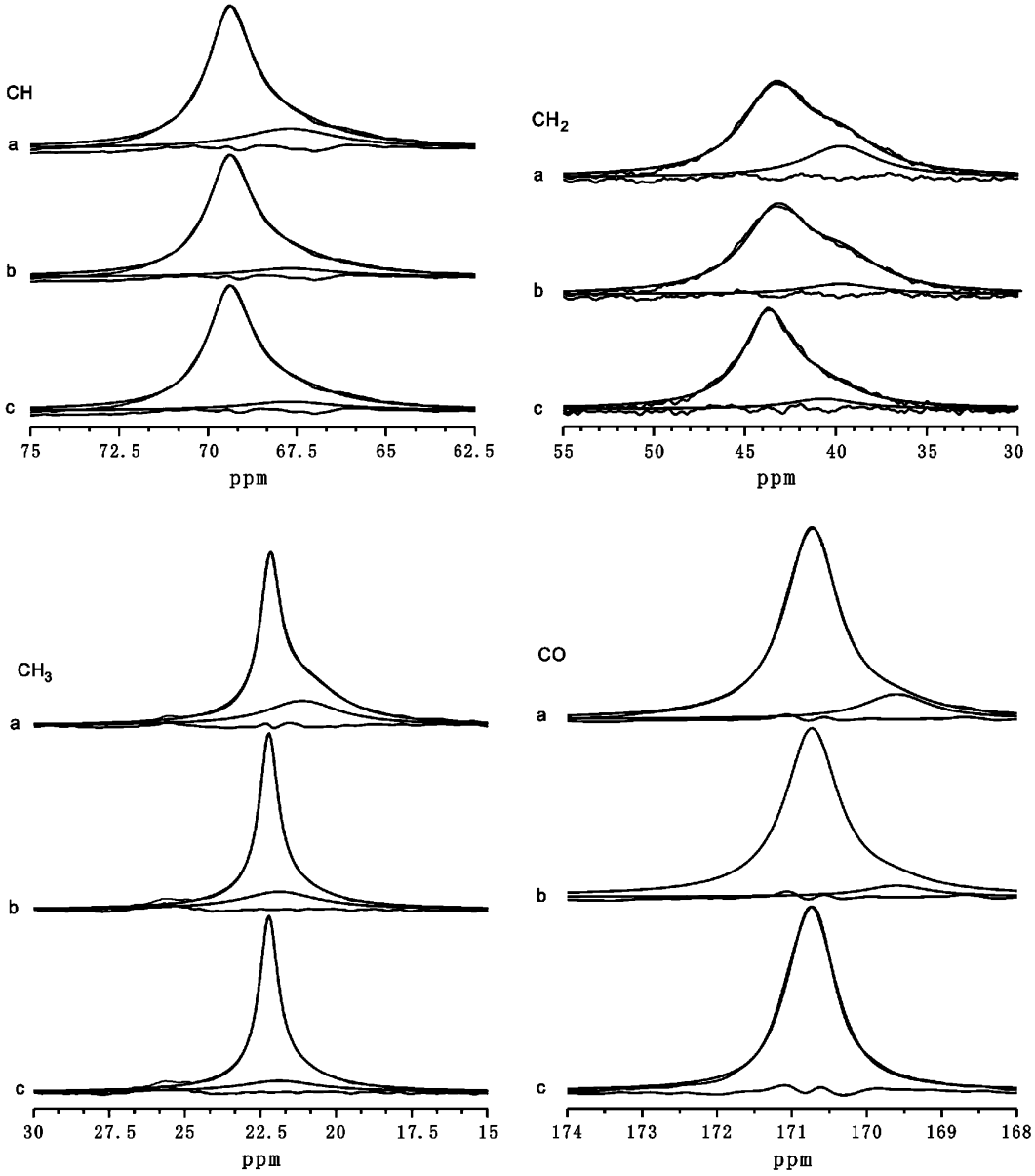

Fig. 5. ^{13}C PRISE spectra of PHB for the expansion of CH, CH_2, CH_3 and C═O groups: (a) normal CPMAS spectrum with contact time of 0.8 ms, (b) ^1H $T_{1\rho}$ based CPMAS NMR spectrum with the relaxation delay (τ_{SL}) of 30 ms, (c) LGFM–CPMAS NMR spectrum with the relaxation delay (τ_{SL}) of 150 ms.

slow decay components is more than an order of magnitude longer than that for the fast decay components. This offers a good opportunity to assign the ^1H $T_{1\rho}$ components with structural details using the PRISE techniques. In our case, PRISE experiments (Fig. 5) revealed that the long ^1H $T_{1\rho}$ components have a set of sharp signals in the CPMAS NMR spectra thus are associated with the crystalline structures whereas the short ones are associated with a set of broad signals assigned to the amorphous regions.

For the H $T_{1\rho}^T$, two components are also present for all three biopolymers (Table 1), both of which are clearly longer than those in the normal ^1H $T_{1\rho}$. This is not surprising since dipole–dipole interactions were the major relaxation driving force; weakening of the dipole–dipole interactions by the Lee–Goldburg sequence is expected to reduce relaxation efficiency and thus increase the relaxation time. This is also consistent with the observations made elsewhere [37]. The difference between two components for H $T_{1\rho}^T$ is also greater than that for ^1H $T_{1\rho}$. The combination of the Lee–Goldburg sequence with frequency modulation (LGFM) [35] with cross-polarization, as shown in Fig. 2c, was used as a spectral editing approach. In this case, the proton magnetization was initially spin-locked at the magic angle by a LGFM sequence in the place of normal spin-locking as in the case of normal $T_{1\rho}$ (Fig. 2b). The results showed that, for all three biopolymers, the long $T_{1\rho}^T$ component is associated with the sharp signals corresponding to the ordered structure whereas the short component is associated with the disordered structure. The advantage of $T_{1\rho}^T$-induced spectral editing method over the $T_{1\rho}$-induced ones is that greater difference between two

components enables spectral editing to be done more conveniently especially for the systems having two $T_{1\rho}$ components.

Above all, the conventional spectral editing methods as well as the newly proposed spectral editing methods enable us to confirm the assignments of the two structure domains present in all three biopolymers. These results may provide structural characteristics and some preliminary information of their dynamic properties. Such properties in the molecular level may in turn provide molecular basis for understanding the thermal properties, such as glass transition (T_g) and melting temperature (T_m), and physical properties. Ultimately, correlation of the molecular information with the thermal and physical properties will be crucial for these biopolymers and their functionality in applications. The results of such studies of the molecular dynamics of these biopolymers are to be reported elsewhere.

3.4. Wide-line proton NMR and domain sizes in PHB and PHBV

The static wide-line ^{1}H solid-state NMR spectra of all three biopolymers showed a narrow signal superimposed on top of a broad resonance (Fig. 6). When the proton spectra of each sample were decomposed into a Gaussian and a Lorentzian line, the full-width at half height ($\Delta\nu_{1/2}$) and the areas of these peaks were obtained. The $\Delta\nu_{1/2}$ values for PHB, PHBV2.7 and PHBV6.5 were about 2.3, 1.9 and 1.5 kHz for the sharp peak (Fig. 6) and 28.6, 27.4 and 24.6 kHz for the broad signal, respectively. The broad peak accounted for about 98.8%, 97% and 86.7% of the whole proton signals for PHB, PHBV2.7 and PHBV6.5. These values are clearly much greater than the X_c values obtained from the ^{13}C SPEMAS NMR results, suggesting that whilst the narrow signal, in general, corresponds to the mobile component with disordered structure, the broad signal corresponds at least partially to the component also with disordered structure with relatively slow motions. In fact only those protons with motions faster relative to the half line-width (30 kHz or $\tau_c \ll 10^{-5}$ s) will be observed as narrow lines, such disordered structures are expected in the amorphous samples below or close to its T_g. It is worth noting that, in theory, when the sample temperature is well above T_g of the amorphous components and below T_m of the crystalline components, X_c values may also be obtained by deconvoluting the static proton spectra.

Domain sizes of both the crystalline and amorphous regions can be determined *via* ^{1}H spin-diffusion measurements provided the diffusion coefficients and domain geometries are known. For the ordered structure that is generally in the rigid regime, the ^{1}H spin-diffusion coefficient [45] (D_s) is typically 1 nm^2/ms (i.e., $\sim 10^{-11}$ cm^2/s). Proton T_1 of these three polymers was single exponential, suggesting that the spin diffusion was efficient on T_1 time scale. On the other hand, ^{1}H $T_{1\rho}$ showed two components, indicating that the spin diffusion was not efficient on the $T_{1\rho}$ time of scale. Therefore, the upper and lower limits of the crystalline domain size can be estimated from the T_1 and $T_{1\rho}$ data. XRD results have shown that PHB and PHBV have lamellar arrangement for their crystalline regions [43]. For PHB, the ^{1}H T_1 value was about 1.2 s and the upper limit for the crystalline domain size is estimated to be 76 nm using the formula [44] $\langle|d|\rangle = (6D_sT_1)^{1/2}$. With the

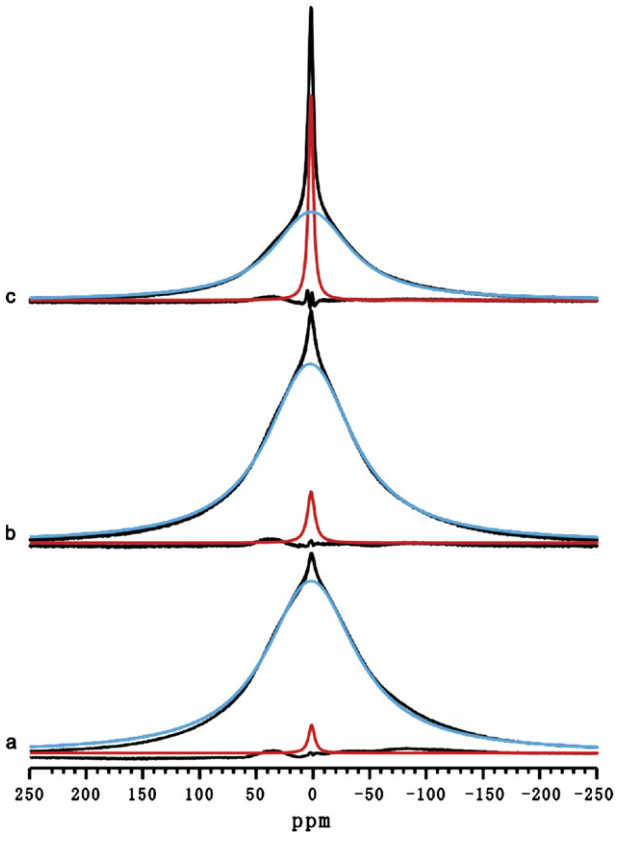

Fig. 6. Static ^{1}H solid-state NMR spectra of (a) PHB, (b) PHBV2.7 and (c) PHBV6.5 at 294 K. The blue and red peaks denote resonant signals associated with crystalline and amorphous components, respectively. (For interpretation of the references to colour in this figure legend, the reader is referred to the web version of this article.)

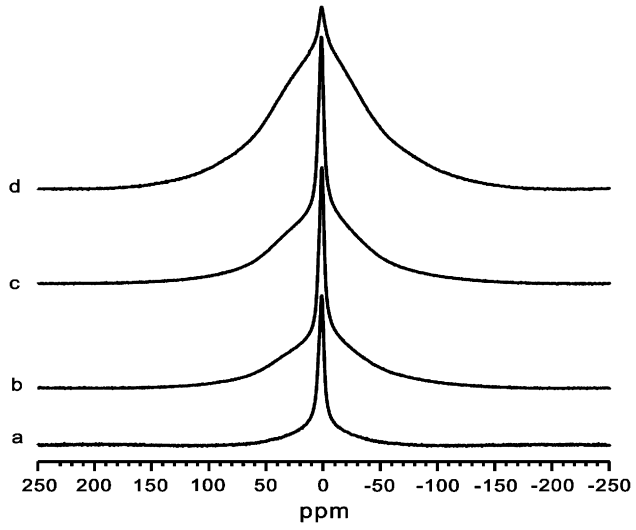

Fig. 7. Static ^{1}H NMR spectra of PHB obtained from the Goldman–Shen sequence at 294 K with the mixing time t_m of (a) 0.1 ms, (b) 10 ms, (c) 50 ms and (d) 300 ms.

long ^{1}H $T_{1\rho}$ values on the scale of 100 ms, the lower limit for the crystalline domain size of the rigid component is estimated to be about 15 nm. In the same way, the estimated crystalline domain sizes were in the range of 12–65 nm and 11–55 nm for PHBV2.7 and PHBV6.5, respectively. To our best knowledge, the domain size data for these polymers have not been reported before.

For the mobile components, the spin-diffusion coefficients have to be measured to estimate the domain sizes, which can be readily done by using the classical Goldman–Shen sequence [40]. When the mixing time was 0.1 ms $< t_m <$ 10–20 ms, the beginning part of the spin-diffusion curves has a linear slope and the intensity at $t_m = 0$ ms can be easily extrapolated from the first data points of the spin-diffusion curve [45]. Proton spectra recorded after different mixing times using Goldman–Shen sequence are shown in Fig. 7 for PHB. The flow of longitudinal magnetization from the mobile domain into the rigid domain is obviously observed with increasing mixing time (0.1, 10, 50 and 300 ms). Fig. 8 shows the spin-diffusion curves for PHB, PHBV2.7 and PHBV6.5 plotted as the normalized intensity of the mobile components as a function of the square root of t_m. As described in the previous work [46,47], the beginning part of the ^{1}H spin-diffusion curve for our polymers is also linear with respect to the root of the mixing time. The domain size of the mobile components can be calculated from the interception of the aforementioned linear decay to the horizontal axis, $t_m^{s,0}$, according to the Fick's second law (Eq. (1)) [46],

$$d_{\text{mobile}} = \frac{2\varepsilon}{\sqrt{\pi}}\sqrt{D_{\text{eff}} t_m^{s,0}} \tag{1}$$

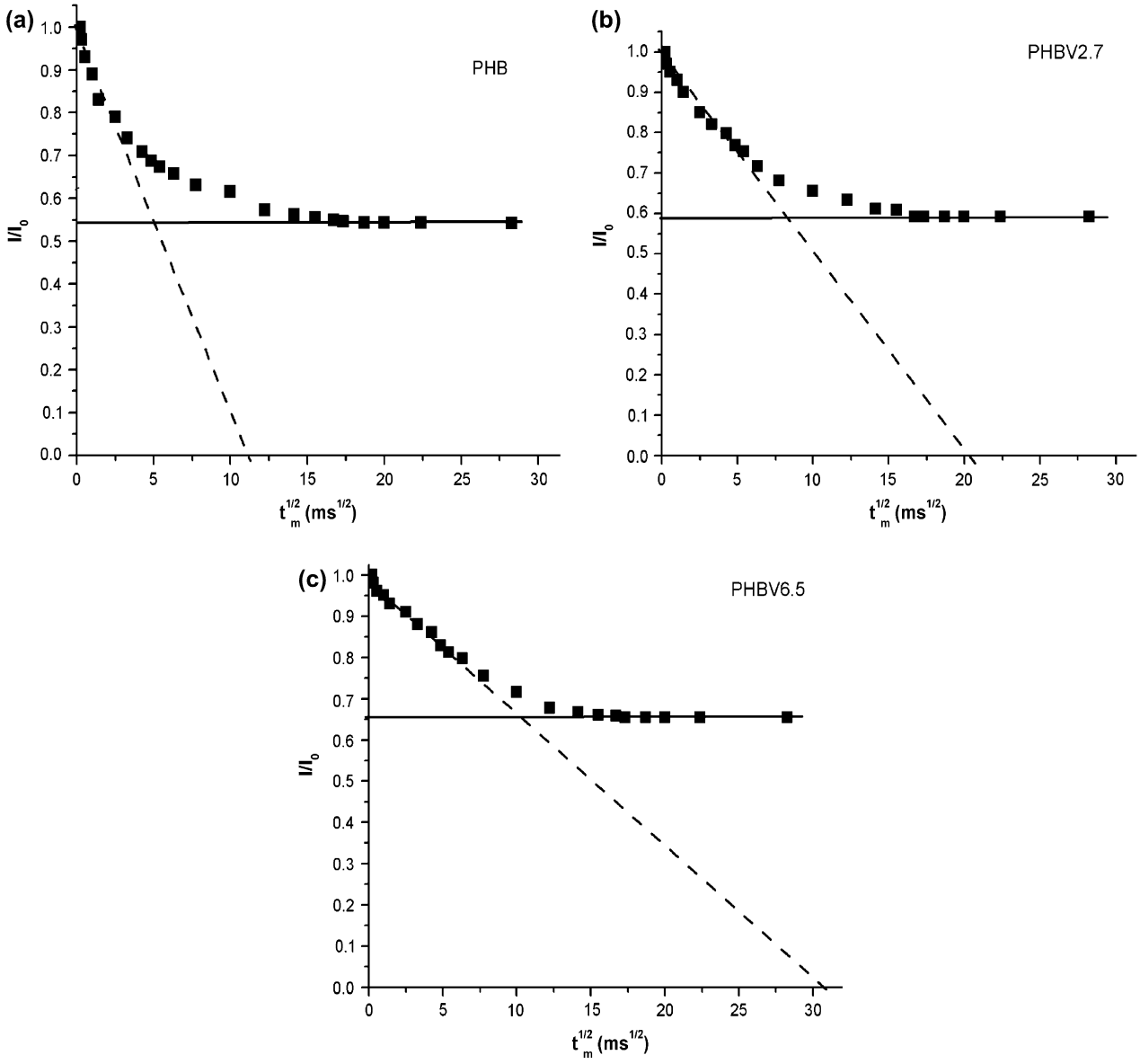

Fig. 8. ^{1}H spin-diffusion curves plotted as the normalized intensity against the square root of the mixing time for (a) PHB, (b) PHBV2.7 and (c) PHBV6.5 at 294 K. The solid and dotted lines denote the plateau values and the $(t_m^{s,0})^{1/2}$ values fitted by a linear equation, respectively.

where ε is the number of orthogonal directions relevant for the efficient spin-diffusion decay. For PHB, PHBV2.7 and PHBV6.5, the XRD [43] results showed that they have lamellar morphology, with polymer chains running perpendicular to the crystallographic c-axis, thus the value of ε is 1 for our biopolymers. The effective spin-diffusion coefficient D_{eff} can be calculated using Eq. (2) [45,46,48–50],

$$\sqrt{D_{\text{eff}}} = \frac{2\sqrt{D_{\text{mobile}} D_{\text{rigid}}}}{\left(\sqrt{D_{\text{mobile}}} + \sqrt{D_{\text{rigid}}}\right)} \tag{2}$$

where D_{rigid} is about 1 nm^2/ms for the typical organic crystalline materials [45,46]. The previous studies [41] showed that the D_{mobile} values correlate empirically with T_2 values, which can be measured with the classical CPMG sequence. When the T_2 values meet the condition of $0 < 1/T_2 < 1000$ Hz and the spin-diffusion coefficient (in nm^2/ms) can be obtained as described [46] in Eq. (3)

$$D(1/T_2) = (8.2 \times 10^{-6} T_2^{-1.5} + 0.007)\ \text{nm}^2/\text{ms} \tag{3}$$

When the $1/T_2$ values are between 1000 and 3600 Hz, their relationship obeys an empirical relationship as described [46] in Eq. (4).

$$D(1/T_2) = (4.4 \times 10^{-4} T_2^{-1} + 0.26)\ \text{nm}^2/\text{ms} \tag{4}$$

From the diffusion curves (Fig. 8), $(t_{\text{m}}^{s,0})^{1/2}$ values for three samples can be obtained [46] by fitting the initial linear points into a linear equation (e.g. $y = ax + b$) (dotted line in Fig. 8). The values are about 11 ms$^{1/2}$, 20.5 ms$^{1/2}$ and 31.5 ms$^{1/2}$ for PHB, PHBV2.7 and PHBV6.5, respectively. The D_{eff} values for PHB, PHBV2.7 and PHBV6.5 are 1.11, 1.07 and 1.01 nm/ms$^{1/2}$, respectively. The mobile domain sizes calculated from Eq. (1) are about 13, 24 and 36 nm for PHB, PHBV2.7 and PHBV6.5, respectively (Table 1). From these data, it is apparent that the introduction of HV leads to the increase of the domain size of the mobile part in the biopolymers. The exact reasons for this dependence remain unknown.

The I/I_0 values at plateau (solid line) of the spin-diffusion curve, in theory, denote the relative ratio of the mobile and rigid domains in the biopolymers [46]. As shown in Fig. 8, these values are 0.54 ± 0.02 for PHB, 0.58 ± 0.02 for PHBV2.7 and 0.66 ± 0.02 for PHBV6.5. The X_c values calculated from these ratios are 65%, 63% and 60% for PHB, PHBV2.7 and PHBV6.5, respectively, which are only about 3–4% lower than the results from the ^{13}C SPEMAS NMR data. This small discrepancy probably results from the inaccuracy of peak deconvolution and the presence of interfaces between the rigid and mobile regions. Nevertheless, the dependence of X_c values on the HV content is consistent with the NMR results discussed in Section 3.2.

4. Conclusion

A catalogue of solid-state NMR methods employed in this study has shown that solid-state NMR is a powerful tool for probing the structure and dynamics of the polyhydroxyalkanoate biopolymers and for providing the structural details of the domains in different dynamic states. Both homopolymer PHB and its copolymers PHBV containing 2.7 mol% and 6.5 mol% HV are composed of amorphous and crystalline regions having distinct dynamics. Such heterogeneity is related to the monomer composition, which is similar to most of the semi-crystalline polymers. As a result, there are two ^{1}H $T_{1\rho}$ components present and the long component is associated with the crystalline regions whereas the short one to the amorphous regions. ^{1}H spin-diffusion measurements concluded that the domain sizes of these two regions are in the range of 15–76 nm, 12–65 nm and 11–55 nm for the crystalline regions of PHB, PHBV2.7 and PHBV6.5, respectively, whilst the mobile domain sizes are 13 ± 2, 24 ± 2 and 36 ± 1 nm for PHB, PHBV2.7 and PHBV6.5, respectively. With ^{13}C SPEMAS NMR, the crystallinity of them was determined as 68%, 60% and 56% for PHB, PHBV2.7 and PHBV6.5, respectively. In addition, it has been observed that introduction of HV enhanced molecular mobility of the biopolymers, raising the ratios of the amorphous regions as a function of increased HV content. Furthermore, conventional PRISE techniques were shown useful in relating structure details to the different dynamics states indicated by the relaxation times. Moreover, our newly proposed spectral editing method based on the H $T_{1\rho}^T$ difference was also efficient in separating signals from two different domains.

Acknowledgements

We acknowledge the financial supports from the State Key Laboratory of Magnetic Resonance and Atomic and Molecular Physics (T152307) and National Natural Science Foundation of China (20425311 and 20575074). H.R.T. also acknowledges financial supports from the Chinese Academy of Sciences for the 100T programme (2005[35]-T12508). Liu Wuyang and Yuan Hanzheng are acknowledged for their technical assistance and hardware managements.

References

[1] Reddy CSK, Ghai R, Rashmi, Kalia VC. Bioresour Technol 2003;87:137–46.
[2] Doi Y. Microbial polyesters. New York: VCH; 1990.
[3] Anderson AJ, Dawes EA. Microbiol Rev 1990;54:450–72.
[4] Madison LL, Huisman GW. Microbiol Mol Biol Rev 1999;63:21–53.
[5] Prud'homme RE, Marchessault RH. Macromolecules 1974;7:541–5.
[6] Prud'homme RE. J Polym Sci Polym Phys Ed 1974;12:2455–63.
[7] Feughelman M. J Appl Polym Sci 1966;10:1937–47.
[8] Hocking PJ, Marchessault RH. Biopolyesters. In: Griffin GJL, editor. Chemistry and technology of biodegradable polymers. London: Chapman & Hall; 1994. p. 48–96 and references therein.
[9] Volova T, Shishatskaya E, Sevastianov V, Efremov S, Mogilnaya O. Biochem Eng J 2003;16:125–33.
[10] Pouton CW, Akhtarb S. Adv Drug Delivery Rev 1996;18:133–62.
[11] Akhtar S, Pouton CW, Notarianni LJ. Polymer 1992;33:117–26.
[12] El-Taweel SH, Hohne GWH, Mansour AA, Stoll B, Seliger H. Polymer 2004;45:983–92.

[13] Gunaratne LM, Shanks RA, Amarasinghe G. Thermochim Acta 2004;423:127–35.
[14] Orts WJ, Marchessault RH, Bluhm TL, Hamer GK. Macromolecules 1990;23:5368–70.
[15] Pazur RJ, Hocking PJ, Raymond S, Marchessault RH. Macromolecules 1998;31:6585–92.
[16] Doi Y, Tamaki A, Kunioka M, Nakamura Y, Soga K. Appl Microbiol Biotechnol 1988;28:330–4.
[17] Kamiya N, Yamamoto Y, Inoue Y, Chûjô R, Doi Y. Macromolecules 1989;22:1676–82.
[18] Shi F, Ashby RD, Gross RA. Macromolecules 1997;30:2521–3.
[19] Shimamura E, Scandora M, Doi Y. Macromolecules 1994;27:4429–35.
[20] Dieter A, Eveline P, Paul F, Jean PR, Peter A, Liesbet S, et al. Polymer 2005;46:2338–45.
[21] Hiroyuki K, Yukari N, Tomoki E, Mitsuo T. Polymer 2004;45:2843–52.
[22] Litvinov VM, Soliman M. Polymer 2005;46:3077–89.
[23] Naoko K, Minoru S, Yoshio I, Riichirô C, Yoshiharu D. Macromolecules 1991;24:2178–82.
[24] Bloembergen S, Holden DA, Hamer GK, Bluhm TL, Marchessault RH. Macromolecules 1986;19:2865–71.
[25] Gunaratne LMWK, Shanks RA. Eur Polym J 2005;41:2980–8.
[26] Kunioka M, Tamaki A, Doi Y. Macromolecules 1989;22:694–7.
[27] Nozirov F, Fojud Z, Klinowski J, Jurga S. Solid State Nucl Magn Reson 2002;21:197–203.
[28] Wang Y, Yamada S, Asakawa N, Yamane T, Yoshie N, Inoue Y. Biomacromolecules 2001;2:1315–23.
[29] Yoshie N, Saito M, Inoue Y. Macromolecules 2001;34:8953–60.
[30] Yoshie N, Menju H, Sato H, Inoue Y. Macromolecules 1995;28:6516–21.
[31] VanderHartt DL, Orts WJ, Marchessault RH. Macromolecules 1995;28:6394–400.
[32] Tang HR, Wang YL, Belton PS. Solid State Nucl Magn Reson 2000;15:239–48.
[33] Tang HR, Hills BP. Biomacromolecules 2003;4:1269–76.
[34] Torchia DA. J Magn Reson 1978;30:613–6.
[35] Hartmann SR, Hahn EL. Phys Rev 1962;128:2042–53.
[36] Sullivan MJ, Maciel GE. Anal Chem 1982;54:1606–15.
[37] Fu R, Jun H, Timothy AC. J Magn Reson 2004;168:8–17.
[38] Carr HY, Purcell EM. Phys Rev 1954;94:630–8.
[39] Meiboom S, Gill D. Rev Sci Instrum 1958;29:688–91.
[40] Goldman M, Shen L. Phys Rev 1966;144:321–31.
[41] Bluhm TL, Hamer GK, Marchessault RH, Fyfe CA, Veregin RP. Macromolecules 1986;19:2871–6.
[42] Chen Y, Yang G, Chen Q. Polymer 2002;43:2095–9.
[43] Marchessault RH, Kawada J. Macromolecules 2004;37:7418–20.
[44] Demco DE, Johansson A, Tegenfeldt J. Solid State Nucl Magn Reson 1995;4:13–38.
[45] Schmidt-Rohr K, Spiess HW. Multidimensional solid state NMR and polymers. San Diego: Academic Press; 1994.
[46] Mellinger F, Wilhelm M, Spiess HW. Macromolecules 1999;32:4686–91.
[47] Spiegel S, Landfester K, Lieser G, Boeffel C, Spiess HW, Eidam N. Macromol Chem Phys 1995;196:985–93.
[48] Mellinger F, Wilhelm M, Landfester K, Spiess HW, Haunschild A, Packusch J. Acta Polym 1998;49:108–15.
[49] Clauss J, Schmidt-Rohr K, Spiess HW. Acta Polym 1993;44:1–17.
[50] Mellinger F, Wilhelm M, Belik P, Schwind H, Spiess HW. Macromol Chem Phys 1999;200:2454–60.